Earthquake Engineering, Tenth World Conference © 1992 Balkema, Rotterdam. ISBN 90 5410 060 5

Seismic hazard prediction using neural nets

Felix S.Wong
Weidlinger Associates, Inc., Los Altos, Calif., USA
Albert T.Y.Tung
San Jose State University, Calif., USA
Weimin Dong
Risk Management Software, Mountain View, Calif., USA

ABSTRACT: This paper presents the development of an adaptive and non-parametric Modified Mercalli Intensity (MMI) forecast model for the direct prediction of spatial distribution of MMI corresponding to an earthquake scenario for use in regional seismic hazard/risk assessment. The development of the model is based on recent advances in Artificial Neural Networks. The neural net based MMI forecast model was constructed through supervised learning utilizing historical earthquakes and regional geological data as training sets. A MMI forecast model for moderate earthquakes with magnitudes between 6 and 7 was developed based on data from several recent California earthquakes. The results demonstrated the generic synthesis capability of a neural net based MMI forecast model and the potential of this model to significantly simplify and improve the seismic hazard/risk assessment methodologies in use today.

1 INTRODUCTION

Current seismic hazard/risk analysis methodologies, both deterministic and probabilistic, employ the peak ground acceleration (PGA) as the ground motion amplitude parameter for measuring the severity of earthquake ground motion. While PGA is very useful from a designer's point of view, it is not strongly correlated to observed structural performance (Campbell, 1985) and is not the parameter used in damage assessment. In general, the PGA is first attenuated from the earthquake source to a site and then is converted to MMI for damage evaluation (Araya and Kiureghian, 1988). Both steps, the attenuation and the PGA-MMI conversion, involve large uncertainties (Murphy and O'Brien, 1977 and Trifunac and Brady, 1975).

This paper presents a new model for the direct prediction of spatial or regional distribution of MMI corresponding to an earthquake scenario based on recent advances in Parallel Distributed Processing or Artificial Neural Networks (NN). In particular, this paper presents the construction of a neural net based MMI forecast model for the prediction of MMI distribution using data from historical earthquakes and regional geological data. The primary advantages of this approach are: First, through the use a neural net to predict directly the spatial distribution of MMI, the seismic hazard/risk analysis methodology is properly consolidated; the two steps mentioned above are combined logically into one and uncertainties are reduced. Second, it presents a solution to the MMI distribution/attenuation relationship in the form of a non-parametric and non-functional model, i.e., the MMI forecast model is optimized without the constraint of an a priori functional form. Third, unlike the multivariate regression approach typically used to model attenuation, the proposed approach allows more variables (e.g., geological data) influencing the MMI distribution to be included in the development of the MMI distribution predictor without any substantial increase in computational complexity. Fourth, the neural net MMI distribution model is extremely flexible and its non-functional, incremental and updatable nature is conducive to improvements of the model as more data become available.

2 ARTIFICIAL NEURAL NETWORKS

Artificial Neural Networks or Parallel Distributed Processing is a recently developed information processing technique (McCelland and Rumelhart, 1988). It is based on computer simulation of the living ner-

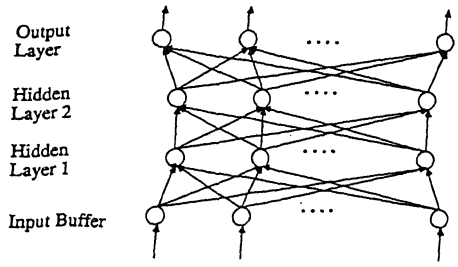

Figure 1: Schematic diagram of a neural net: connected processing elements arranged in layers.

vous system. Neural computing processes information through interactions involving large numbers of simulated neurons or processing elements (PE). A neural net consists of many PEs joined together and is typically structured in the form of a sequence of layers with full or random connections between successive layers. In general, for each neural net, there are two layers serving as buffers. There is an input buffer (layer) where data is presented to the network and an output buffer (layer) which holds the response of the network to a given set of input. Layers distinct from the input and output layers are called the hidden layers. Figure 1 shows the schematic diagram of a typical net.

One of the more powerful and popular neural network paradigms is the back-propagation net (McCelland and Rumelhart, 1986) which is employed in this study. The typical back-propagation net always has an input layer, an output layer, at least one hidden layer, and each layer is fully connected to the succeeding layer. The input into each PE in the back-propagation network is processed as follows:

$$x_j^{(s)} = f\left(\sum(w_{ji}^{(s)} * x_i^{(s)-1})\right) = f(I_j^{(s)}) \qquad (1)$$

where $x_j^{(s)}$ is the current output of the jth PE in layer s; $w_{ji}^{(s)}$ is the weight on connection joining the ith PE in layer $(s-1)$ to the jth PE in layer s; $I_j^{(s)}$ is the weighted summation of input to the jth PE in layer s; and $f(\cdot)$ is a transfer function. The transfer function is traditionally the sigmoid function, $f(z) = (1+e^{-z})^{-1}$, but can be any differentiable function such as the Hyperbolic tangent, $f(z) = (e^z - e^{-z})/(e^z + e^{-z})$.

The dynamic modification of the connection weights, $w_{ji}^{(s)}$, is based on the so called Delta Rule which minimizes the global error, E, through changing each connection weight according to the size and direction of negative gradient on the global error surface, i.e., $\triangle w_{ji}^{(s)} = -lcoef * (\partial E/\partial w_{ji}^{(s)})$ where $lcoef$ is a learning coefficient.

The back-propagation network is very powerful for constructing non-linear transfer functions between several continuously valued inputs and one or more continuously valued outputs. However, it requires much supervised training with lots of input-output examples. In addition, there is no guarantee

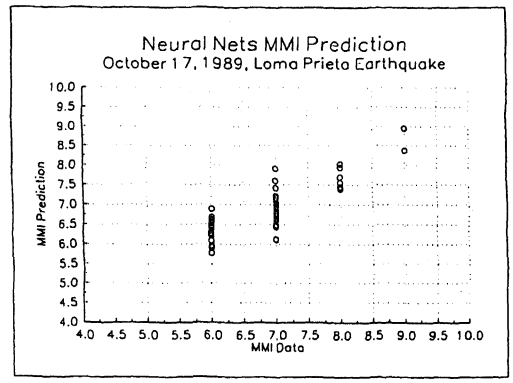

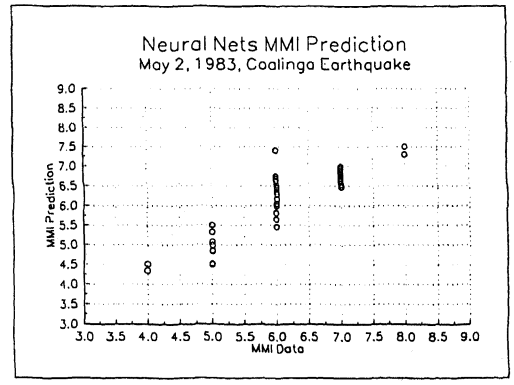

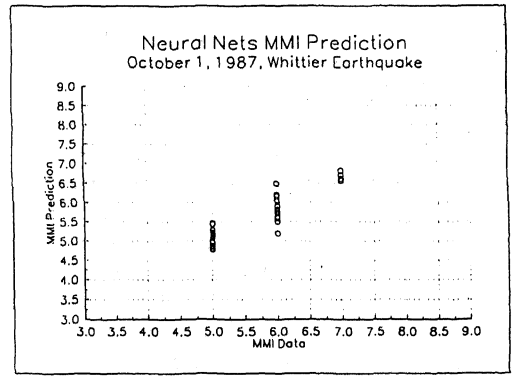

Figure 2: Predicted vs. desired MMI values from three individually trained nets.

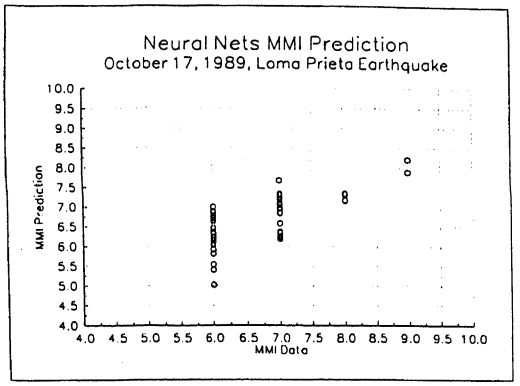

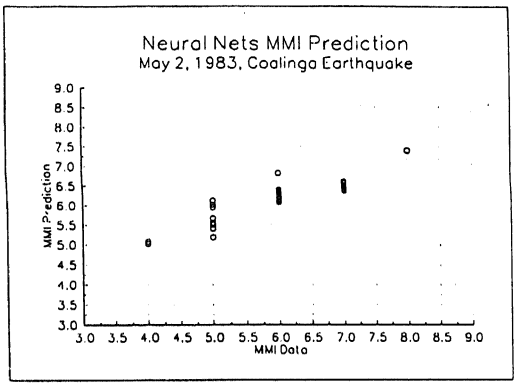

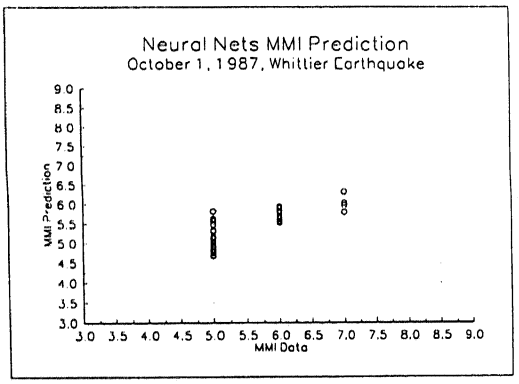

Figure 3: Predicted vs. desired MMI values for three earthquakes from output of a single net.

that the system will converge, and convergence is one of the important questions investigated in this study.

3 NEURAL NETS MMI PREDICTION

The neural net based MMI forecast model requires training using damage data from historical earthquakes. Three recent California earthquakes were selected to provide the necessary input. They are (1) Loma Prieta (LP) earthquake of 17 October 1989 ($M_L = 7.0$); (2) Coalinga (CO) earthquake of 2 May 1987 ($M_L = 6.7$); and (3) Whittier Narrows (WN) earthquake of 1 October 1987 ($M_L = 6.1$). There are several reasons for their selection. First, damages due to these earthquakes are well documented. Second, all three earthquakes occurred in areas where geological conditions or maps are available. Third, the magnitudes of the three earthquakes span the range of 6 to 7 which allows an investigation of the generic synthesis capability of the resulting (trained) neural nets.

A number of attributes are needed as input to train the neural net model. Four attributes are attached to each recorded MMI location and they are (1) the Richter magnitude of the earthquake event; (2) the shortest distance from the site to the fault rupture (plane); (3) the azimuth angle formed by the shortest distance (line) and the fault rupture (plane); and (4) the local geological condition. In determining the azimuth angle, a straight line approximating the fault rupture (plane) is taken as the axis. Although azimuth angle has a range of 0 to 360 degrees, the normalized azimuth angle used as an input attribute is converted to a range of 0 to 90 degrees according to the equations below:

$$\alpha' = \begin{cases} \alpha, & 0 < \alpha \leq 90 \\ 180 - \alpha, & 90 < \alpha \leq 180 \\ \alpha - 180, & 180 < \alpha \leq 270 \\ 360 - \alpha, & 270 < \alpha \leq 360 \end{cases} \quad (2)$$

where α' is the normalized azimuth angle. In addition, the local geologic condition is differentiated into three categories with 1 = rock, 2 = alluvium, and 3 = Bay Mud.

The strong-motion recording stations maintained by California Strong Motion Instrumentation Program (CSMIP) with their precise locations known are chosen as sites where MMI levels are determined for the recorded seismic events. For each CSMIP station, a MMI level is combined with the set of four input attributes to form an input-output pair and the pair is used as a training set in the supervised training mode during the construction of the neural net MMI forecast model. There are 72, 58 and 67 training sets for the LP, CO and WN earthquakes, respectively.

The basic form of the MMI forecast model is the back-propagation neural net consisting of one input layer (4 nodes), one output layer (1 node) and one hidden layer (6 nodes). All nodes are fully connected to the nodes of adjacent layers. The learning

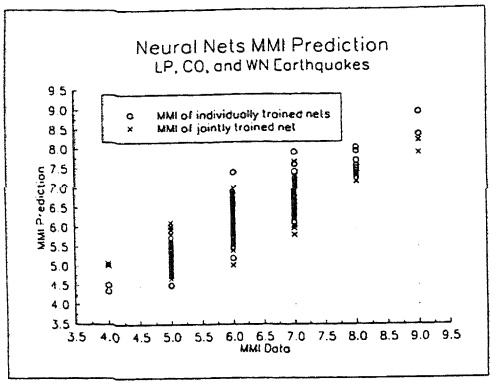

Figure 4: Comparison of predicted vs. desired MMI values between three individually trained nets and a jointly trained net.

rule and transfer function combination employed is the Normalized Cumulative-Delta-Rule and the Hyperbolic Tangent pair. They have been found to be efficient for the particular type of data analyzed.

During the training process, records are selected randomly from the data set and one "pass" of the data file is completed when all the records of the data set are processed. Many passes are usually required to train the network to reach a desired level of prediction accuracy. For this study, in general, 30,000 to 50,000 passes of the data sets are necessary for the construction of the MMI forecast models.

Although the goal of this study is to construct a neural net based MMI forecast model to predict the spatial distribution of MMI for scenario earthquakes of various magnitudes, the first step, however, was the determination of the pattern-attribute relationships or the correlations between the MMI spatial distribution and its corresponding input attributes of the individual earthquake events. Using the data sets of the individual earthquakes (LP, CO, and WN), three neural net based MMI forecast models were constructed. Then employing the combined data from all three earthquakes, a single neural net MMI forecast model was built.

After each neural net is fully trained, a recall test is performed. In the recall test, only the input attributes only of the training sets are shown to the neural net and the neural net predicts the MMI. The predicted MMI is then compared with the desired value. As mention previously, neural nets were first constructed singly using data sets of individual earthquakes. Figure 2 shows the comparison between the predicted and the desired MMI values

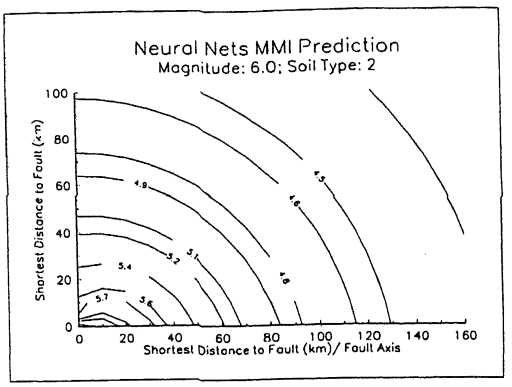

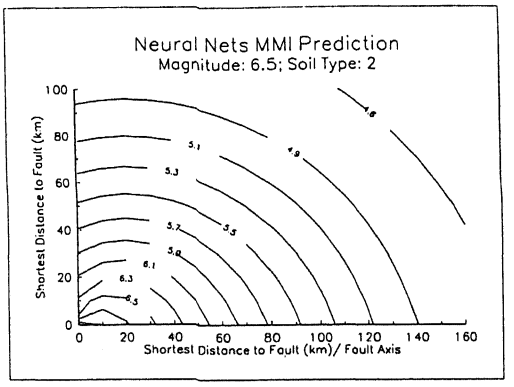

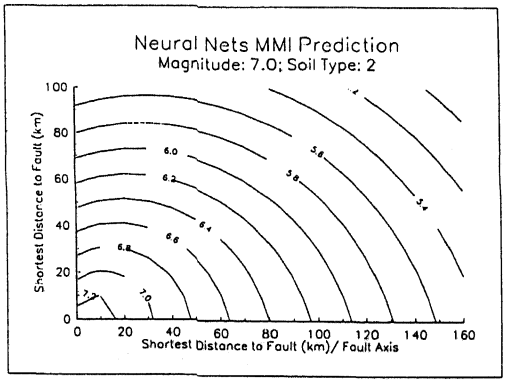

Figure 5: Contour Plots of MMI spatial distribution for azimuth angles between 0 and 90 degrees (alluvium sites and M_L = 6.0, 6.5, and 7.0).

from the three individually trained MMI forecast models based on LP, CO, and WN data sets.

Although input MMI levels are discrete numbers, the output is in the form of continuous numbers. If the predicted value is considered satisfactory when it falls within the range of ± 0.5 MMI of the desired MMI values, then the three neural nets

have successful recall rates of 78%, 83% and 97% for LP, CO and WN earthquakes, respectively. The overall predictive capability of the neural net MMI forecast models appears to be quite adequate.

Next, using the combined data set (197 records), a single neural net MMI forecast model was built for the prediction of MMI distribution of earthquakes with Richter magnitudes in the range of 6 to 7. The recall results of this neural net in predicting MMI when given individually the attributes associated with the three earthquakes used in training is shown in Figure 3. Figure 4 shows a comparison of the predicted output MMI values from the individually trained nets and the jointly trained net for the three earthquakes used in the study. The jointly trained net seems to be slightly less accurate than the singly trained nets in recall mode for predicting MMI at the extreme ends of the MMI range trained.

Since the azimuth angle was expected to have an effect on the distribution of MMI level, it was included as one of the input attributes. The results, as expected, showed a pattern/correlation between the azimuth angle and MMI levels. Figure 5 shows the spatial distribution pattern of MMI for the azimuth angle range of 0 to 90 degrees. The plots are for alluvium sites. However, it appears to be a general trend that greater attenuation of MMI occurs in the direction perpendicular to the fault rupture plane (axis).

4 CONCLUSIONS

It is shown in this paper that a neural net based MMI forecast model can be satisfactorily used to predict the spatial distribution of MMI for moderate earthquakes. The neural net model successfully associates the key features such as magnitude, distance, azimuth angle, and soil condition with the MMI levels.

The neural net approach, being non-parametric, non-functional, and adaptive, is fundamentally different from other approaches such as regression analysis. Although this paper presents a MMI forecast model for earthquakes with magnitudes limited within the range of 6 to 7, results of the study indicate that the realization of a neural net MMI forecast model for a much wider magnitude range is quite promising.

The proposed MMI model when incorporated into the current seismic hazard/risk analysis procedures will in essence combine two steps, the attenuation of PGA and the PGA-MMI conversion, into one. Thus, it represents both a simplification and improvement of the seismic hazard/risk assessment methodologies in use today.

REFERENCES

[1] Rodrigo Araya and Armen Der Kiureghian. *Seismic Hazard Analysis: Improved Models, Uncertainties and Sensitivities.* Earthquake Engineering Research Center Report UCB/EERC-90/11, University of California, Berkeley, 1988.

[2] Kenneth W. Campbell. Strong motion attenuation relations: a ten year perspective. *Earthquake Spectra*, 1(4), 1985.

[3] James L. McCelland and David E. Rumelhart. *Explorations in Parallel Distributed Processing.* MIT Press, Cambridge, Massachusetts, 1988.

[4] J. R. Murphy and L. J. O'Brien. The correlation of peak ground acceleration amplitude with seismic intensity and other physical parameters. *Bulletin of the Seismological Society of America*, 67, 1977.

[5] Yoh-Han Pao. *Adaptive Pattern Recognition and Neural Networks.* Addison-Wesley, New York, 1989.

[6] David E. Rumelhart and James L. McCelland. *Parallel Distributed Processing: Exploration in the Micro- structure of Cognition, Volume 1.* MIT Press, Cambridge, Massachusetts, 1986.

[7] M. D. Trifunac and A. G. Brady. On the correlation of seismic instensity scales with the peaks of recorded strong ground motion. *Bulletin of the Seismological Society of America*, 65, 1975.